Stability of Global Alfvén Waves (TAE, EAE) in JET Tritium Discharges

W Kerner, D Borba, G T A Huysmans, F Porcelli,
S Poedts[1], J P Goedbloed[1], R Betti[2].

JET Joint Undertaking, Abingdon, Oxon, OX14 3EA.
[1] FOM Institute for Plasma Physics, 'Rijnhuizen', Nieuwegein, The Netherlands.
[2] Lab. Laser Energetics, Un. Rochester, Rochester, USA.

STABILITY OF GLOBAL ALFVÉN WAVES (TAE, EAE) IN JET TRITIUM DISCHARGES

W. Kerner, D. Borba, G.T.A. Huysmans, F. Porcelli, S. Poedts*,
J.P. Goedbloed* and R. Betti**

JET Joint Undertaking, Abingdon, Oxon, OX14 3EA, UK
*FOM Institute for Plasma Physics, 'Rijnhuizen', Nieuwegein, The Netherlands
**Lab. Laser Energetics, Un. Rochester, Rochester NY 14627, USA

The study of MHD modes driven unstable by energetic particles due to additional heating and, in particular, by alpha particles is crucial for the prediction of α-confinement for future JET D-T discharges aiming at $Q_{DT} \simeq 1$. In this paper we analyse the toroidicity and elongation induced Alfvén eigenmodes (TAE, EAE), their damping and their destabilisation by energetic particles. The spectral code CASTOR (Complex Alfvén Spectrum for Toroidal Plasmas) together with the equilibrium solver HELENA (see ref. [1]) provides the tool for the analysis of the ideal and dissipative MHD spectrum.

The successful production of controlled thermonuclear energy using a deuterium tritium fuel mixture was achieved with the JET tokamak experiment on the 9th November 1991. The total fusion releases were 1.7MW peak power and 2MJ of energy [2]. The α-particle pressure was moderate, $\beta_\alpha = 1.5 \times 10^{-4}$, with a peaked value on axis of $\beta_\alpha(0) = 1.4 \times 10^{-3}$.

Usually, the stable Alfvén branches exhibit continua corresponding to eigenmodes where every field line oscillates with its own local frequency $\omega_A(r) = k_{\|}\ v_A(r)$. If a coherent oscillation is enforced within such a continuum, e.g. by antenna excitation, this 'friction' yields resonant absorption. This effect accounts for the continuum damping. In a toroidal system with a finite aspect ratio the poloidal harmonics are coupled causing gaps in the continua. For further details refer to [1].

The Alfvén spectrum for the JET PTE1 (#26148) for a toroidal wave number n = 1 is displayed in Fig. 1a). Here, the value of the safety factor is above unity, $q(0) = 1.05$, throughout the plasma, which is appropriate for the early stages of the discharge. Since the plasma pressure is not large the Alfvén branch is examined solely; this is done by using a small value for the ratio of the specific heats. Two gaps are important, the toroidicity induced at $\omega / \tilde{\omega}_A = 0.5$ ($\approx$ 150kHz) and the elongation induced gap at $\omega / \tilde{\omega}_A = 1.0$; $\tilde{\omega}_A$ denotes the characteristic Alfvén frequency at the magnetic axis. The TAE/EAE are localised around the flux surface where $k_{\|m,n} = -k_{\|\tilde{m},n}$, which corresponds to a value of the safety factor at the gap position

$$q_G = \frac{m + \tilde{m}}{2n} = \left(\frac{3}{2} \text{for } m = 1,\ \tilde{m} = 2 \text{ and } n = 1 \right). \tag{1}$$

For this X-point discharge with nearly parabolic density profile there are radially four gaps. Furthermore, four discrete eigenmodes exist in each of the major gaps. Two are strongly damped but the remaining two TAE and EAE exhibit no continuum damping because the gaps corresponding to different poloidal mode numbers m thread through the plasma. For a high density pedestal near the plasma boundary, here simulated by the extreme case of constant density (broken lines in Fig. 1a), the gaps are shifted relatively to each other. This yields finite damping. The magnitude of this continuum damping strongly depends on the magnitude of the singular component. In particular, the continuum damping for the discrete mode with frequency $\omega / \tilde{\omega}_A = 0.30$ is still weak - $\gamma/\omega_G = 10^{-3}$. Only for the discrete EAE with frequency $\omega / \tilde{\omega}_A = 1.0$, where the continuum couples to the leading harmonics, the damping is large $-\gamma/\omega_G = 6 \times 10^{-3}$.

The Alfvén continua for n = 3 are displayed in Fig. 1b). Since the mode width, Δ_n, of the discrete eigenmodes becomes narrower with increasing mode numbers $(\Delta_n \sim 1/n)$, the interaction with the continua occurs dominantly in the side harmonics. This yields decreasing continuum damping. A residual damping due to the Landau interaction with thermal electrons and ions, electron collisions, etc. can be offset by the inverse Landau damping with alpha particles, resulting in unstable global Alfvén modes.

The result of Betti and Freidberg for the growth rate takes into account the α-particle drive and the background electron and ion Landau damping

$$\gamma / \omega_G = q_G{}^2\{\beta_\alpha(nq_G\delta_\alpha H_\alpha - G_\alpha) - 0.5\ \beta_c(G_i + G_e)\}, \qquad (2)$$

where the functions H_α, G_α, G_i and G_e together with the normalised α-pressure gradient length δ_α are defined in the paper [3].

Evidently, the alpha drive initially increases linearly with n up to an optimal number corresponding to the radial mode width becoming of the order of the radial alpha particle orbit width, $\Delta_b \sim q\rho_\alpha$. In JET, where $\Delta_b \sim$ 5-10 cm the condition $\Delta_b \le \Delta_n$ is satisfied typically for $n \le 5$. These conditions lead us to conclude that Alfvén gap modes with toroidal mode numbers $n \ge 5$ are very hard to excite in foreseen JET DT experiments.

The gap structures and continuum damping for perturbations with n = 1 to 5 have been investigated. An example of the gap structure for n = 3 is shown in Fig. 1b), using the plasma parameters, in particular the density and q profiles, of the JET discharges #26148 (PTE1) and #26087 (JET best performance). From this preliminary study, the mode numbers have been selected which appear as most dangerous according to the following criteria: i) minimal or absent continuum damping; ii) "robust" gaps in the sense of surviving small changes (within estimated error bars) of the density and q profiles; iii) gaps located within 0.6 of the minor radius. In fact, the resonant α-particle contribution is most significant near the gap location and β_α drops to a negligible value for $r/a \ge 0.6$.

Marginal stability curves for the selected mode numbers have been obtained with a separate code based on the approximation used by Betti and Freidberg, Eq. (2). This analysis yields that the toroidicity - induced Alfvén gap eigenmode (TAE) with $n = 3$, and dominant poloidal harmonics $m = 3, 4$ is the most dangerous one for the parameters of these two discharges. In particular, for the PTE1 experiment, we have utilised the actual experiment values of deuterium, tritium and impurity densities. In the second case corresponding to the best performance in JET (#26087), we have simulated results assuming an equal concentration of deuterium and tritium. In both cases the alpha pressure profile has been evaluated by TRANSP which includes beam-beam and beam-plasma thermonuclear reactions, as well as thermal-thermal reactions.

The results of our analysis are summarised in Figs. 3 and 4, showing marginal stability curves in the $\beta_{\alpha G}$ - v_α/v_{AG} plane for the $n = 3$, $m = 3, 4$ TAE mode. Here v_{AG} and $\beta_{\alpha G}$ denote the Alfvén velocity and alpha particle beta at the gap location where $q_G = (m+1/2)/n = 7/6$, which is estimated to be at $r_G/a = 0.47 \pm 0.04$. The impurity mass density is included in the definition of v_A, while $v_\alpha = (2\varepsilon_\alpha/m_\alpha)^{1/2}$ with $\varepsilon_\alpha = 3.5\text{MeV}$. The hatched regions in Figs. 2 and 3 reflect the sensitivity of the marginal stability curves to uncertainties in the gap location, the electron and ion temperatures at the gap, and the α-particles pressure scale length, $L_\alpha = -(d\ln p_\alpha/dr)^{-1}{}_G$. The experimental values of these parameters (with error bars) are indicated in the figure captions. The figures also show the estimated values of $\beta_{\alpha G}$ and v_α/v_{AG} at the time corresponding to the maximum of $\beta_{\alpha G}$. Note that for both cases $\beta_\alpha(0)/\beta_\alpha(r_G) \sim 10$.

The conclusion from this analysis is that α-particle driven global Alfvén modes were stable in the PTE1 experiment and should be stable also in PTE2 provided the same ion density as in #26087 (which is higher than that in PTE1) is obtained. However, the proximity of the relevant parameters to their marginal stability values indicates that the excitation of Alfvén gap modes in future JET experiments is a realistic possibility. In particular, on the basis of Fig. 3, the unstable domain may be accessed in future D-T experiments by operating at lower plasma density and higher ion temperatures. In this fashion the ratio v_α/v_{AG} can be decreased to its optimal value for instability while maintaining a significant level of alpha particle production.

If the losses together with the mode amplitude and the effective plasma damping can be established experimentally, firm predictions about α-particle confinement and, possibly, scenarios for ash removal will become feasible.

REFERENCES

[1] S. Poedts, W. Kerner, J.P. Goedbloed, B. Keegan, G.T.A. Huysmans and E. Schwarz in Plasma Phys. and Cont. Fusion **34**, 1397 (1992).

[2] JET Team, Nucl. Fusion **32** (2), 197 (1992).

[3] R. Betti and J.P. Freidberg, Phys. Fluids **34**, 1465 (1992).

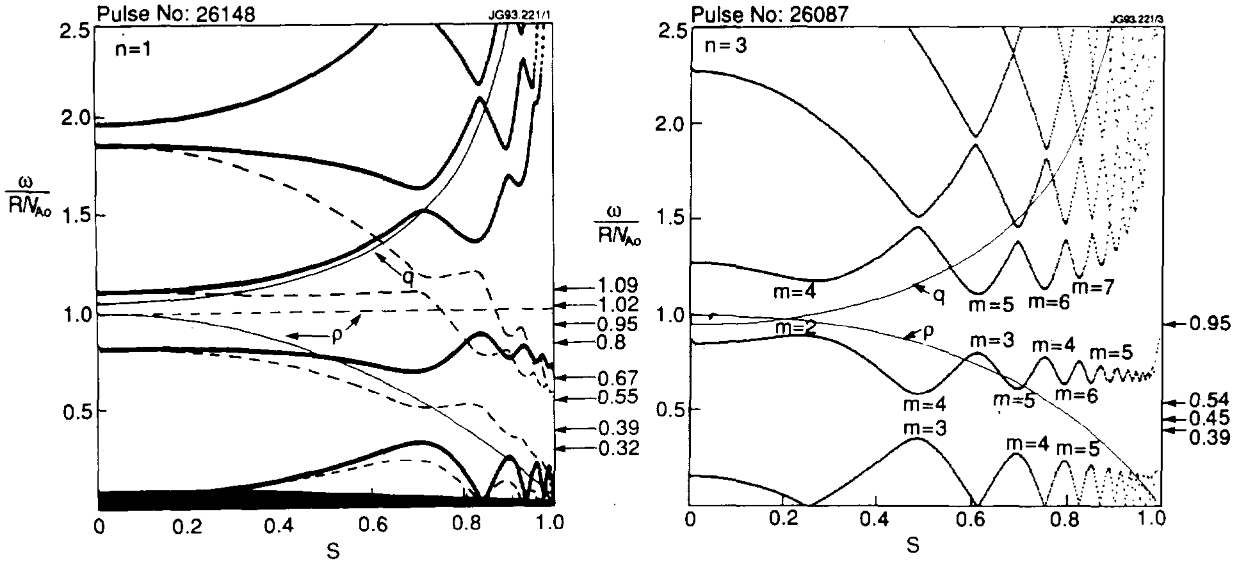

Fig 1. The radial dependance, $s = \sqrt{\Psi / \Psi s}$, of the ideal MHD Alfvén continuous spectrum of a typical JET PTE1 discharge. The global Alfvén eigenmodes are indicated by arrows a) n = 1 and b) n = 3.

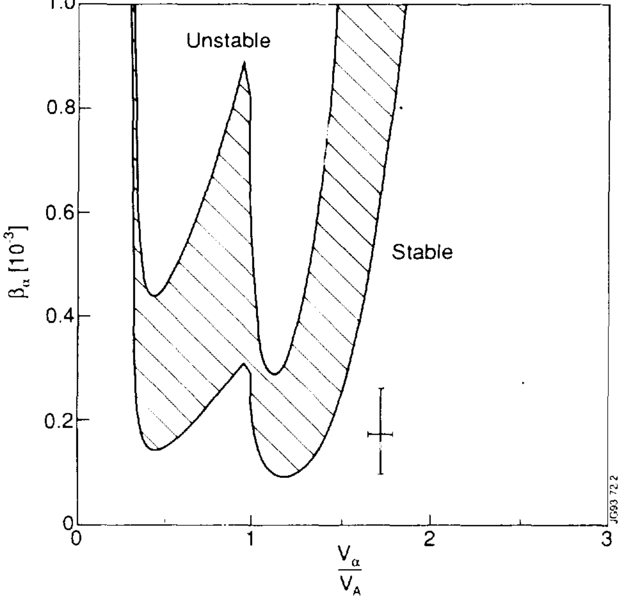

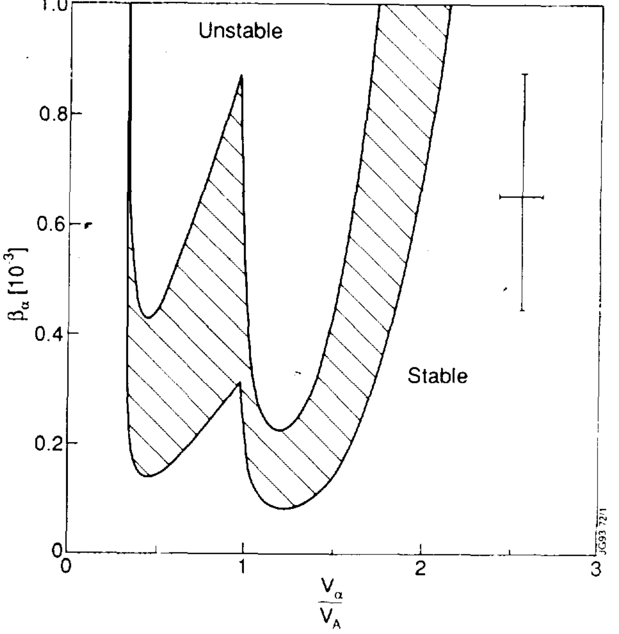

Fig. 2 Stability boundary for discharge #26148 for the TAE mode with n = 3 and dominant m = 3 and 4 harmonics.

Fig. 3 Stability boundary for discharge #26087 for the TAE mode with n = 3 and dominant m = 3 and 4 harmonics assuming $n_D \sim n_T$.

Parameters at the $q_G = 7/6$ surface which is at $r_G/a = 0.47 \pm 0.04$ are as follows ($B_T = 2.8T$): #26148: $n_e = (3 \pm 0.3) \times 10^{19}$; $n_D = (1.84 \pm 0.2) \times 10^{19}\ m^{-3}$; $n_T = (0.2 \pm 0.02)\ 10^{19}\ m^{-3}$; $T_i = (11 \pm 1)$ keV; T_e (7.5 ± 0.5) keV; $L_\alpha/a = 0.15 \pm 0.05$; $\beta_\alpha = (1.7 \pm 0.7) \times 10^{-4}$.
#26087: $n_e = (4.8 \pm 0.04) \times 10^{19} m^3$; $n_D = (1.8 \pm 0.02) \times 10^{19}\ m^{-3}$; $n_T = (1.9 \pm 0.02)\ 10^{19}\ m^{-3}$; $n_I = (1.8 \pm 0.2) \times 10^{18} m^{-3}$, $T_i = (9.5 \pm 0.5)$ keV; $T_e = (8.2 \pm 0.5)$ keV; $L_\alpha/a = 0.15 \pm 0.05$; $\beta_\alpha = (6.5 \pm 2.5) \times 10^{-4}$. The hatched region reflects the sensitivity of the marginal stability curve to variations of the relevant parameters within the corresponding error bars. The indicated values of $\beta_{\alpha G}$ and v_α/v_{AG} corresponds to the maximum value of β_α during the discharge evolution.